Low-profile Circularly Polarized Conformal Antenna Array with Side Lobe Suppression for Vehicular SATCOM Applications

Ebenezer Abishek[1], Ramesh Subramaniam[2], Parthasarathy Ramanujam[3], and Manikandan Esakkimuthu[4]

[1]Department of Electronics and Communication Engineering
Vel Tech Multi Tech Dr.Rangarajan Dr.Sakunthala Engineering College, Chennai, 600062, India
ebenezerabishek@gmail.com

[2]Department of Electronics and Communication Engineering
SRM Valliammai Engineering College, Chennai, 603203, India

[3]Department of Electronics and Communication Engineering
National Institute of Technology, Tiruchirappalli, 620015, India

[4]Centre for Innovation and Product Development
Vellore Institute of Technology, Chennai, 600127, India

***Abstract* –** A circularly polarized microstrip antenna array with low side lobe levels is proposed for Vehicular Satellite Communication. The suppression of side lobe levels is accomplished by the non-uniform power distribution utilized to feed the individual patch elements. Impedance matching is ensured by the incorporation of a quarter-wave transformer via a microstrip line fed to the edge of the patch. When the proposed amplitude-weighted feed is compared to the conventional corporate feed, simulation results indicate a reduction in side lobe levels of 8.9 dB. The proposed antenna is constructed out of RT/DUROID 5880 material, which is lighter, more flexible, and less expensive than ceramic materials. The radiation characteristics of the proposed antenna are compared when the antenna is planar versus when it is made to conform to the roof of the vehicle. The measured results indicate a reflection coefficient at the resonant frequency of -31.5 dB and -27.7 dB when conformal, an impedance bandwidth of 410 MHz and 180 MHz when conformal, an axial ratio bandwidth of 140 MHz and 170 MHz when conformal, and a peak gain of 15.719 dB and 14.335 dB when conformal. The measured results validate the simulation results that this proposed antenna is appropriate for a variety of Vehicular Satellite Communication applications.

***Index Terms* –** amplitude tapering ratio, circular polarization, microstrip array, side lobe level, vehicular satellite communication.

I. INTRODUCTION

The vehicle-based SATCOM technology is known as Vehicular Satellite Communication. Satellites are utilized to establish and maintain communication between moving vehicles and immobile infrastructures such as hospitals, police stations, etc. Compared to vehicle-to-vehicle communication, the satellite provides a larger coverage area in vehicular satellite communication [1]. Important issues that must be addressed in Vehicular Satellite Communication include interference with nearby satellites [2], [3] and the need for increased power to provide high-quality services [4], [5]. Due to their ability to overcome the Faraday rotation that occurs in the ionosphere, circularly polarized antennas are preferred for Vehicular Satellite Communications [6], [7]. The radiation characteristics of a microstrip antenna with a single element can be enhanced by constructing an array of that antenna.

Microstrip technology is used to develop the proposed antenna as a low-profile alternative to conventional SATCOM antennas. IEEE has established Wireless Access in Vehicular Environment as the standard for vehicular networks [8], [9]. This standard is a part of the IEEE 802.11p protocol for mobile ad hoc networks. Vehicular Satellite Communication necessitates the installation of antennas on moving vehicles. More than 50% of earth-orbiting satellites are used for communication [10], [11]. Among these satellites there are satellites used exclusively for Vehicular Satellite Communication to connect moving vehicles and also to

Submitted On: October 21, 2022
Accepted On: July 1, 2023

https://doi.org/10.13052/2023.ACES.J.380608

stationary infrastructures [12], [13]. There are numerous civilian applications, including the use of laptops or mobile devices with high-speed internet connectivity in moving vehicles, rapid rescue of passengers in moving vehicles in the event of an accident, tracking of thieves travelling in moving vehicles in the event of a theft, etc. [14]. Vehicular Satellite Communication antennas are also required for military vehicles to maintain communication with the satellite even when traversing difficult terrain [15], [16]. There is a need for low-profile alternatives to high-profile vehicular antennas because a greater number of antennas must be integrated into vehicles as the number of applications increases [17].

Power is a crucial factor for providing high-quality services in moving vehicles. Therefore, it is undesirable for the side lobes to waste energy. Various techniques can be used to suppress side lobes [18]. To address this issue, it is proposed to implement a feed structure that suppresses the side lobes, thereby reducing the battery's power consumption. This feed structure is incorporated into the proposed planar antenna array alongside circularly polarized patches. The radiation characteristics of this proposed planar antenna array are examined and discussed.

II. ANTENNA DESIGN METHODOLOGY

The antenna proposed was developed in three stages. In the initial phase of the work, a single element microstrip antenna with circular polarization and improved cross polarization isolation is developed. This preliminary phase of the project has been completed and published [19]. A proposed feed structure is designed to suppress the side lobes in the second stage. Using the single element circularly polarized microstrip patch antenna developed in the first stage and the proposed feed structure, a proposed 1*8 element antenna array is constructed. The third stage entails adapting the proposed planar antenna array to the shape of the vehicle's roof. The antenna's dimensions are optimized to compensate for changes in the desired performance caused by the conformal placement of the proposed antenna on the roof of the vehicle. The proposed antenna's radiation characteristics are analyzed using both simulated and measured data.

The proposed feed structure uses unequal T-junction power dividers to distribute power with tapered amplitude. Taylor, Chebyshev, and Binomial arrays are frequently employed amplitude tapered or amplitude weighted arrays, each with their own benefits and drawbacks. Although Binary arrays completely eliminate side lobes, the amplitude coefficients of the array's individual elements vary greatly. If the Taylor array achieves a radiation pattern with complete suppression of inner side lobes and all side lobes at the same level, directivity will decrease. Chebyshev arrays are also used to obtain optimal main lobe and suppressed side lobe radiation patterns. The T-junction used for unequal power distribution is shown in Fig. 1.

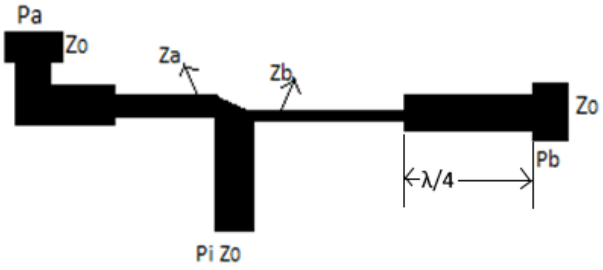

Fig. 1. T-junction unequal power divider.

Assuming lossless transmission, the relation between input and output power of the T-junction power divider for unequal power distribution can be written as

$$P_o = P_a + P_b = P_i, \tag{1}$$

where $P_i = V_o^2/2Z_o$,

$$P_a = V_o^2/2Z_a \text{ and} \tag{2}$$

$$P_b = V_o^2/2Z_b. \tag{3}$$

$$P_a = aP_i. \tag{4}$$

$$P_b = (1-a)P_i, \tag{5}$$

where a value lies between 0 and 1.

The output port impedances derived from the above equations can be written as

$$Z_a = Z_o/a, \text{ and} \tag{6}$$

$$Z_b = Z_o/(1-a). \tag{7}$$

Equation (1) describes the simplest case of unequal power division. The impedance is varied at the output ports because of the different widths of the feed at the output ports. The relation between the impedance at ports and the amount of power division is described in equations (2) and (3). Equations (4) to (7) describe the unequal power division and its relation to impedance. Given that port 1 is matched, the formula for calculating the input time average power is $P_i=V_o{}^2/Z_o$, where V_o is the junction's phasor (total) voltage. Since both ports are assumed to be matched, the output powers can be computed similarly and are given in equations (2) and (3). To achieve the desired distribution of incident power between the two output ports, the characteristic impedances of the two transmission lines are modified. The modified values of characteristic impedances are given in equations (6) and (7). The modified characteristic impedances result in unequal power division, and the ratio of unequal power division is given in equations (4) and (5). If output power is known, the impedance of the T-junction output ports can be determined. Using the above equations, the quarter wave transformer transforms impedance in order to perform

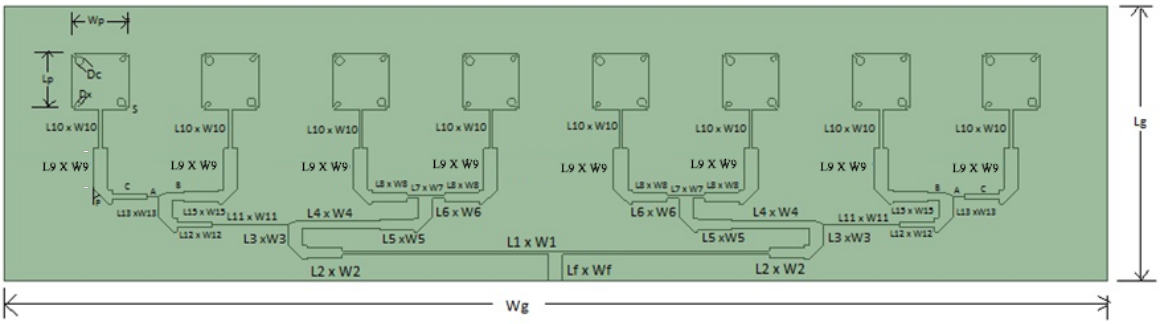

Fig. 2. Design of the proposed planar microstrip array.

power division and determine the physical dimensions of the proposed feed structure [20].

The proposed 1*8 element planar array is constructed using this feed structure and the single element circularly polarized patch antenna array as depicted in Fig. 2. and the optimal physical dimensions of the proposed antenna are given in Table 1.

Table 1: Physical dimensions of the proposed planar microstrip array

Parameters	Values
Lg × Wg	39.23mm × 157.83mm
Lp × Wp	8mm × 8mm
Dc	1.2
Dx	0.69
Lf × Wf	4mm × 2mm
L1 × W1	0.4mm × 60mm
L2 × W2	1.2mm × 4.8mm
L3 × W3	2.4mm × 2mm
L4 × W4	1.1mm × 10.8mm
L5 × W5	1.7mm × 4.9mm
L6 × W6	2.5mm × 2mm
L7 × W7	0.5mm × 5.5mm
L8 × W8	1.4mm × 4.9mm
L9 × W9	7.8mm × 2mm
L10 × W10	5.6mm × 0.4mm
L11 × W11	0.15mm × 11mm
L12 × W12	0.85mm × 4.9
L13 × W13	2.4mm × 1.8mm
L15 × W15	1.6mm × 4.8mm
A	0.25mm × 1.6mm
B	1mm × 1.75mm
C	0.8mm × 4.8mm
D	2mm × 0.5mm
E	2mm × 0.5mm
F	2mm × 0.5mm
G	2mm × 0.5mm
H	2mm × 0.5mm
P	45^o

The unequal power distribution to the individual patch elements is proportional to the 0.5:1:2:2:2:2:1:0.5 amplitude tapering ratio. The power divider at the T-junction is designed for this amplitude tapering ratio. The material chosen for antenna construction is 0.78 mm thick RT Duroid 5880. This substrate material's permittivity measures 2.2. For the construction of the proposed 1*8 element planar antenna array, the circularly polarized single element antenna and the proposed feed structure are combined. This proposed antenna is mounted conformally to the vehicle's roof, as depicted in Figs. 3 and 4, shown below.

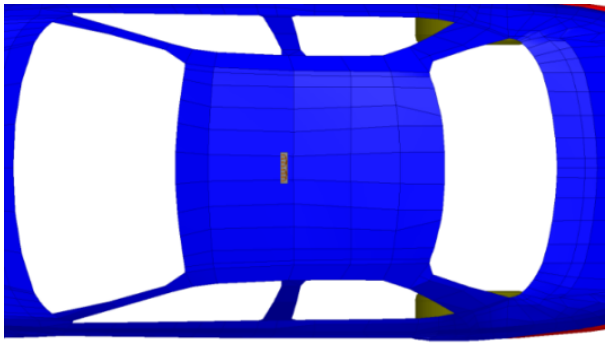

Fig. 3. Proposed conformal microstrip antenna array–top view.

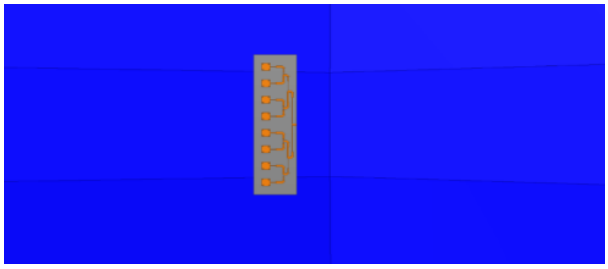

Fig. 4. Magnified top view of conformal microstrip antenna array.

The conformal placement of the proposed antenna reduces its visibility to human eyes and improves its mechanical properties, such as the reduction of aerodynamic drag. The rise in the number of antennas mounted on civilian vehicles makes the conformal antenna an attractive option for vehicle manufacturers.

III. RESULTS AND DISCUSSION

A. Planar microstrip antenna array proposed for vehicular SATCOM applications

Simulating the proposed antenna utilizes both the HFSS and CST suite tools. The reflection coefficient versus frequency graph is depicted in Fig. 5. The impedance bandwidth at -10 dB is measured using this graph, which is the industry standard. At a resonant frequency of 11.2 GHz, simulation results indicate an impedance bandwidth of 410 MHz, or 3.66% of the resonant frequency. The axial ratio of practically circularly polarized antennas should be less than 3. The axial ratio versus frequency graph is depicted in Fig. 6. This graph is used to evaluate the bandwidth of the axial ratio at 3 dB. Simulated results reveal an axial ratio bandwidth of 150 MHz at a resonant frequency of 11.2 GHz, which is 1.34% of the resonant frequency.

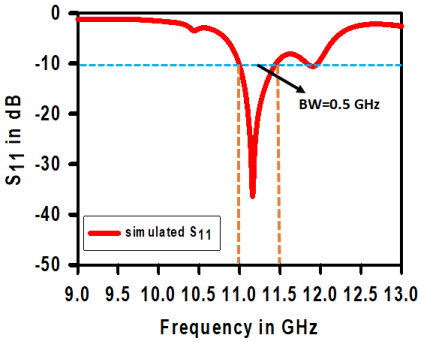

Fig. 5. Return loss versus frequency plot of proposed planar microstrip antenna array.

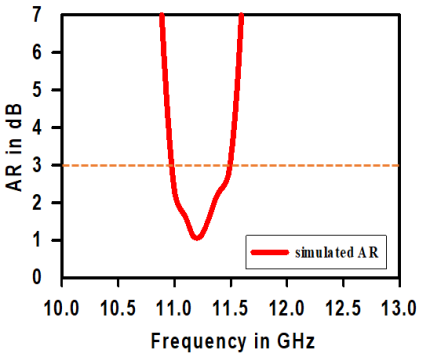

Fig. 6. Axial ratio versus frequency plot of proposed planar microstrip antenna array.

Figure 7 shown below depicts the linear gain versus theta relationship. The graph displays a maximum gain of 14 dB, and the difference in gain between co-polarization and cross-polarization is consistently greater than 15 dB. Figure 8 depicts the polar gain versus theta plot. Maximum gain is 13.54 dB, and the difference between co-polarization and cross-polarization gain is greater than 15 dB throughout the entire plot. Figure 9

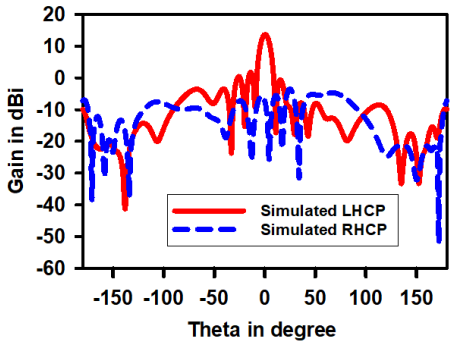

Fig. 7. Polarization gain versus theta linear plot of proposed planar microstrip antenna array.

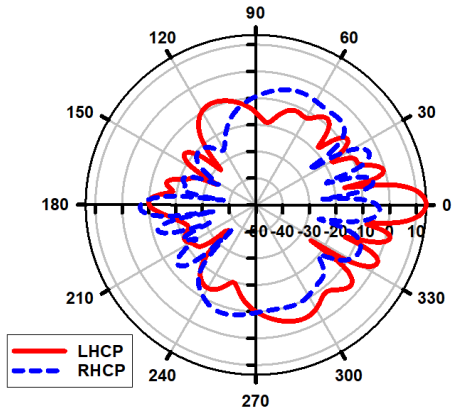

Fig. 8. Polar plot of polarization gain versus theta for proposed planar microstrip antenna.

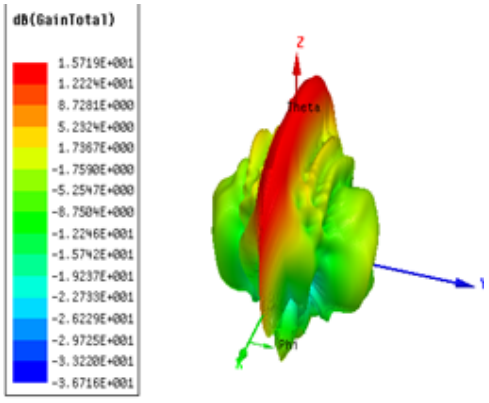

Fig. 9. 3D gain representation of the proposed planar microstrip antenna array.

illustrates the 3D gain versus frequency graph. The graph displays a maximum gain of 15.71 dB.

B. Conformal microstrip antenna array proposed for automotive SATCOM applications

Simulating the proposed antenna utilizes both the HFSS and CST suite tools. Figure 10 depicts a reflection coefficient versus frequency graph. The impedance bandwidth at -10 dB is measured using this graph, which is the industry standard. At the resonant frequency of 11.2 GHz, simulation results indicate an impedance bandwidth of 180 MHz, or 1.6% of the resonant frequency. The axial ratio of practically circularly polarized antennas should be less than 3. The axial ratio versus frequency graph is depicted in Fig. 11. This graph is utilized to assess the axial ratio bandwidth at 3 dB. Simulated results reveal an axial ratio bandwidth of 180 MHz at a resonant frequency of 11.2 GHz, which is 1.6% of the resonant frequency. Figure 12 depicts the graph of 3D gain versus frequency. The graph indicates a peak gain of 14.39 dB.

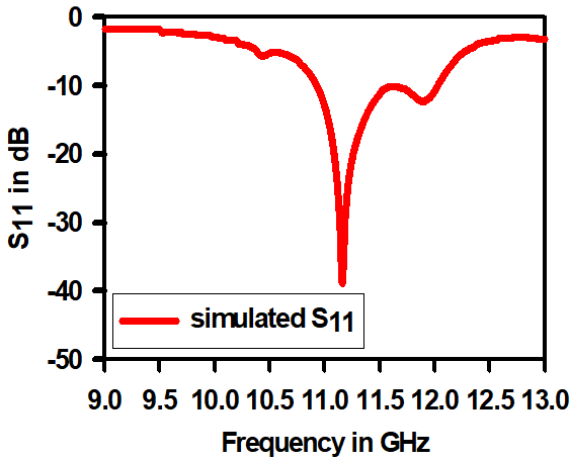

Fig. 10. Conformal microstrip antenna array return loss versus frequency plot.

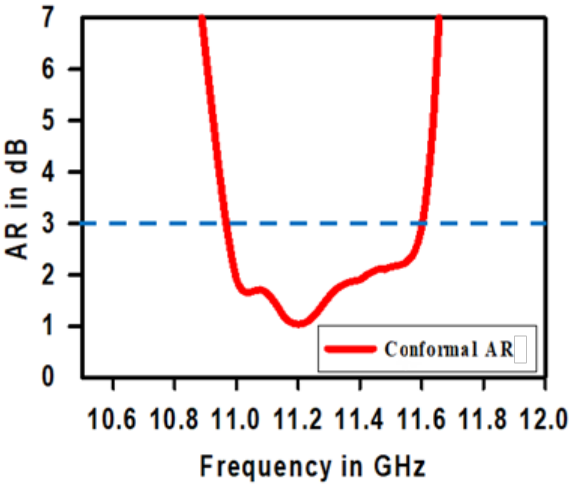

Fig. 11. Conformal microstrip antenna array axial ratio versus frequency plot.

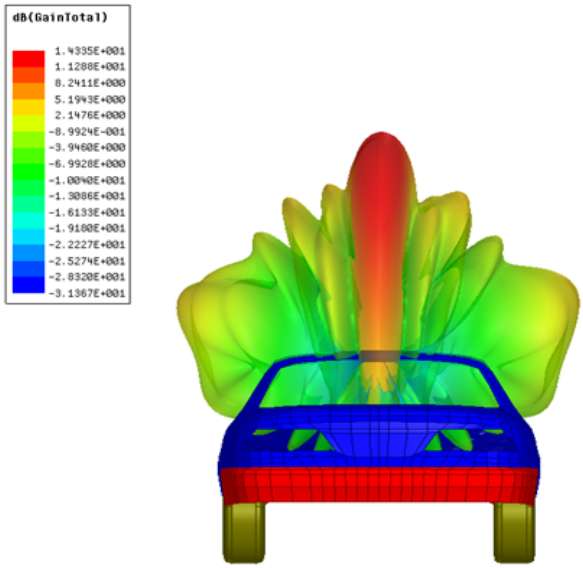

Fig. 12. 3D pattern of proposed conformal microstrip antenna array's far field.

C. Reduced side lobe levels

Figures 13 and 14 depict the far field directivity versus theta plot of the circularly polarized planar array with the existing feed and the proposed feed, respectively. The results demonstrate that the proposed feed's side lobe levels are 8.9 dB lower than the corporate feed.

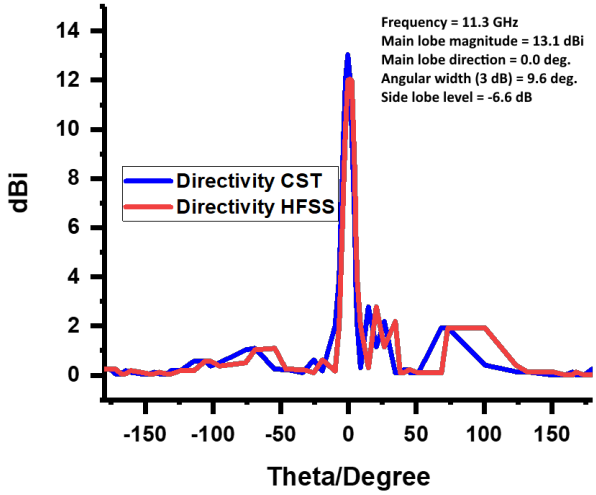

Fig. 13. Side lobe levels of a conventional-feed conformal antenna–directivity in Cartesian plot.

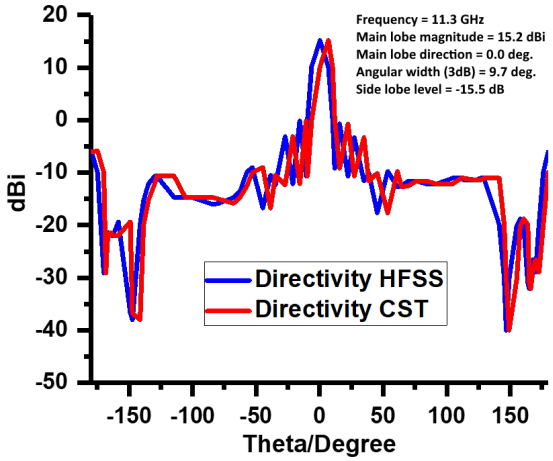

Fig. 14. Side lobe levels of conformal antenna with proposed feed–directivity in Cartesian plot.

D. Fabrication and testing

Figure 15 depicts the developed planar and conformal circularly polarized microstrip array antenna with a single element. These antennas were evaluated by measuring the various parameters of radiation characteristics using a test setup comprised of a transmitting Verdant JR12 horn antenna, Vector Network Analyzer, and anechoic chamber. Figure 16 depicts the proposed antenna

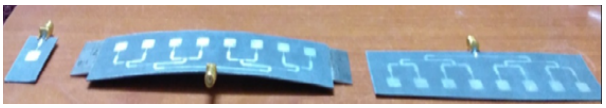

Fig. 15. Single-element proposed planar microstrip antenna array and conformal microstrip antenna array fabrication.

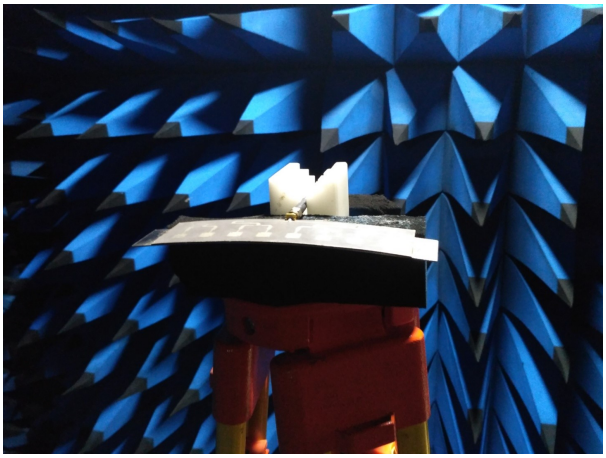

Fig. 16. Testing the proposed conformal microstrip antenna array in the anechoic chamber.

placed in the anechoic chamber for testing. The proposed antenna was measured with the transmitting Verdant JR12 horn antenna positioned at 2 metres distance apart. Figures 17, 18 and 19 depict simulation versus comparison plots for the various radiation characteristic parameters.

The proposed conformal microstrip antenna array is compared with similar antennas in recent research and is shown in Table 3 given above. At the resonant frequency, Figs. 18, 19, and 20 demonstrate good agreement between the simulated and measured values. Although the gain could not be measured directly using the test setup, it was calculated using the Friss transmission formula. Comparing the measured gain to the gain obtained through simulation, connector losses caused a slight decrease in gain. Table 2 provides a comparison between the measured radiation characteristic parameters of single element antenna, proposed planar array and proposed conformal array.

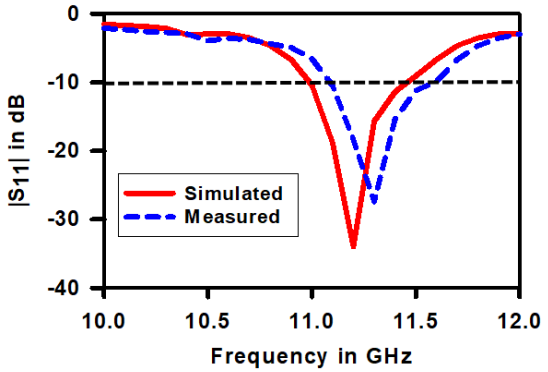

Fig. 17. Simulated versus measured return loss of proposed conformal microstrip antenna array.

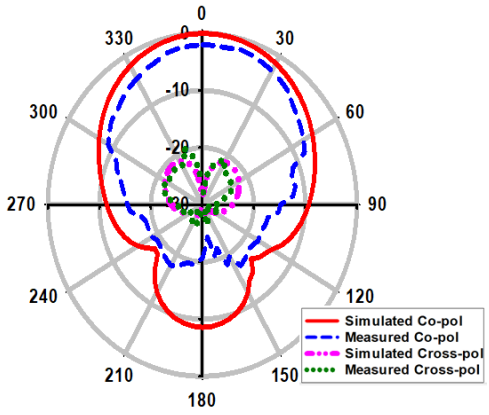

Fig. 18. Radiation pattern in the far field of the proposed conformal microstrip antenna array in the Y-Z plane (E-Plane).

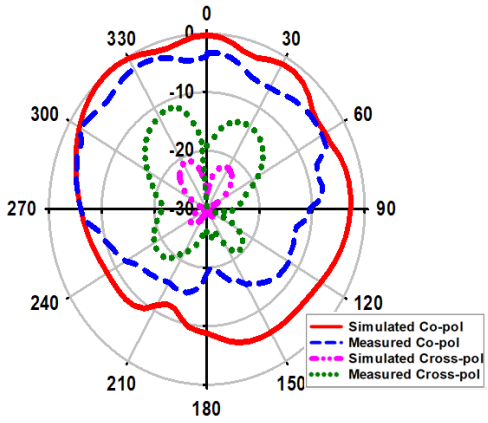

Fig. 19. Radiation pattern in the far field of the proposed conformal microstrip antenna array in the X-Z plane (H-Plane).

Table 2: Comparison of the measured results of single element antenna, proposed planar and proposed conformal microstrip antenna array

Parameter	Single Element Antenna	Proposed Planar Array	Proposed Conformal Array
Impedance Bandwidth (MHz)	490	400	170
Axial Ratio Bandwidth (MHz)	170	140	160
Gain (dB)	5.6	14	13.33

Table 3: Comparison of performance metrics of the proposed antenna with recent related works

Ref.	Resonant Frequency (GHz)	Gain (dBi)	Side Lobe Levels (dB)
[19]	11.2	5.6	−14.9
[21]	13	19.4	−16
[22]	12.2	25.3	<−26.5
[23]	4.3-7.4	5-6.5	around −15
[24]	9.3	11.39	−20
[25]	9.37	28	−25
This work	11.2	14.335	−15.5

IV. CONCLUSION

The proposed microstrip conformal circularly polarized antenna array has been designed, simulated, developed, tested, and measured for vehicular applications. RT 5880 material with a thickness of 0.78 mm was utilized as the substrate. The characteristics of the radiation were analyzed using both simulated and measured data. The proposed feed structure reduces side lobe levels by 8.9 dB compared to the current feed structure. The measured results reveal 1 dB reduction in gain when compared to the simulation findings; however, the measured values are consistent with the simulation findings. According to the measured data, the proposed antenna has a gain of 13.33 dB, an impedance bandwidth of 1.6%, and an axial ratio bandwidth of 1.6%. The proposed antenna's enhanced axial ratio bandwidth and reduced side lobe levels make it the optimal low-profile antenna for vehicular SATCOM applications.

REFERENCES

[1] Z. Zhao, G. Xu, N. Zhang, and Q. Zhang, "Performance analysis of the hybrid satellite-terrestrial relay network with opportunistic scheduling over generalized fading channels," *IEEE Transactions on Vehicular Technology*, vol. 71, no. 3, pp. 2914-2924, Mar. 2022.

[2] H. K. Kim, Y. Cho and, H. S. Jo, "Adjacent channel compatibility evaluation and interference mitigation technique between earth station in motion and IMT-2020," *IEEE Access*, vol. 8, pp. 213185-213205, Nov. 2020.

[3] A. D. Panagopoulos, M. P. Anastasopoulos, and P. G. Cottis, "Error performance of satellite links interfered by two adjacent satellites," *IEEE Antennas and Wireless Propagation Letters*, vol. 6, pp. 364-367, Oct. 2007.

[4] W. Li, Q. Zhang, Y. Luo, Q. Zhang, and F. Jiang, "Development of a new multifunctional induced polarization instrument based on remote wireless communication technology," *IEEE Access*, vol. 8, pp. 100415-100425, May 2020.

[5] L. Liu, Y. Yi, J.-F. Chamberland, and J. Zhang, "Energy-efficient power allocation for delay-sensitive multimedia traffic over wireless systems," *IEEE Transactions on Vehicular Technology*, vol. 63, no. 5, pp. 2038-2047, June 2014.

[6] L. Zhang, S. Gao, Q. Luo, P. R. Young, W. Li, and Q. Li, "Inverted-S antenna with wideband circular polarization and wide axial ratio beamwidth," *IEEE Transactions on Antennas and Propagation*, vol. 65, no. 4, pp. 1740-1748, Apr. 2017.

[7] Y. Yao, F. Shu, Z. Li, X. Cheng, and L. Wu, "Secure transmission scheme based on joint radar and communication in mobile vehicular networks," *IEEE Transactions on Intelligent Transportation Systems*, pp. 1-11, May 2023.

[8] S. A. M. Ahmed, S. H. S. Ariffin, N. Fisal, and S. Com, "Overview of wireless access in vehicular environment (WAVE) protocols and standards," *Indian Journal of Science and Technology*, vol. 6, no. 7, pp. 4994-5001, July 2013.

[9] M. M. Bilgic and K Yegin, "Low-profile wideband antenna array with hybrid microstrip and waveguide feed network for Ku band satellite reception systems," *IEEE Trans. Antennas Propag*., vol. 62, no. 4, pp. 2258-2263, Jan. 2014.

[10] F. Ananasso and F. D. Priscoli, "The role of satellites in personal communication services," *IEEE Journal on Selected Areas in Communications*, vol. 13, no. 2, pp. 180-196, Feb. 1995.

[11] A. I. Zaghloul, R. K. Gupta, E. C. Kohls, L. Q. Sun, and R. M. Allnutt, "Low cost flat antennas for commercial and military SATCOM terminals," *MILCOM Proceedings Communications for Network-Centric Operations: Creating the Information Force (Cat. No.01CH37277)*, vol. 2, pp. 795-799, Oct. 2001.

[12] G. Comparetto and R. Ramirez, "Trends in mobile satellite technology," *Computer*, vol. 30, no. 2, pp. 44-52, Feb. 1997.

[13] B. Cao, J. Zhang, X. Liu, Z. Sun, W. Cao, R. M. Nowak, and Z. Lvet, "Edge-cloud resource scheduling in space-air-ground-integrated networks for internet of vehicles," *IEEE Internet of Things Journal*, vol. 9, no. 8, pp. 5765-5772, Apr. 2022.

[14] S. Jiang, C. Zhao, Y. Zhu, C. Wang, and Y. Du, "A practical and economical ultra-wideband base station placement approach for indoor autonomous driving systems," *Journal of Advanced Transportation*, vol. 2022, pp. 1-12, Mar. 2022.

[15] Y. Li, K. An, T. Liang, and X. Yan, "Secrecy performance of land mobile satellite systems with imperfect channel estimation and multiple eavesdroppers," *IEEE Access*, vol. 7, pp. 31751-31761, Mar. 2019.

[16] C. Chen, S. Wang, L. Li, S. Ke, C. Wang, and X. Bu, "Intelligent covert satellite communication for military robot swarm," *IEEE Access*, vol. 8, pp. 5363-5382, Dec. 2019.

[17] S. Pan, M. Lin, M. Xu, S. Zhu, L.-A. Bian, and G. Li, "A low-profile programmable beam scanning holographic array antenna without phase shifters," *IEEE Internet of Things Journal*, vol. 9, no. 11, pp. 8838-8851, June 2022.

[18] R. Masood and S. A. Mohsin, "No side-lobe condition for linear uniform broadside and end-fire antenna arrays," *IEEE 15th International Symposium on Antenna Technology and Applied Electromagnetics*, Toulouse, France, pp. 1-6, June 2012.

[19] E. Abishek, A. Raaza, S. Ramesh, S. Jerritta, and V. Rajendran, "Circularly polarized circular slit planar antenna for vehicular satellite applications," *Applied Computational Electromagnetics Society (ACES) Journal*, vol. 34, no. 9, pp. 1340-1345, Sep. 2019.

[20] D. M. Pozar and D. H. Schaubert, "Microstrip antenna array design," *Microstrip Antennas: The Analysis and Design of Microstrip Antennas and Arrays*, Wiley-IEEE Press, pp. 267-308, 1995.

[21] U. Beaskoetxea, A. E. Torres-García, M. Beruete, "Ku-band low-profile asymmetric bull's-eye antenna with reduced sidelobes and monopole feeding," *IEEE Antennas and Wireless Propagation Letters*, vol. 17, no. 3, pp. 401-404, Mar. 2018.

[22] L.-X. Wu, N. Zhang, K. Qu, K. Chen, T. Jiang, J. Zhao, and Y. Feng, "Transmissive metasurface with independent amplitude/phase control and its application to low-side-lobe metalens antenna," *IEEE Transactions on Antennas and Propagation*, vol. 70, no. 8, pp. 6526-6536, Aug. 2022.

[23] F. Z. Abushakra, A. S. Al-Zoubi, and D. F. Hawatmeh, "Design and measurements of rectangular dielectric resonator antenna linear arrays," *Applied Computational Electromagnetics Society (ACES) Journal*, vol. 33, no. 4, pp. 380-387, July 2021.

[24] Y. P. Saputra, F. Oktafiani, Y. Wahyu, and A. Munir, "Side lobe suppression for X-band array antenna using Dolph-Chebyshev power distribution," *22nd Asia-Pacific Conference on Communications (APCC)*, Yogyakarta, Indonesia, pp. 86-89, Aug. 2016.

[25] L. Lu, L. Shu, W. Jun, L. Shoulan, Y. Caitian, and A. Denisov, "Simulation and analysis of an X-band low sidelobe and high gain microstrip antenna array," *International Symposium on Antennas and Propagation (ISAP)*, Phuket, Thailand, pp. 1-2, Oct. 2017.

Ebenezer Abishek is an Associate Professor at Vel Tech Multi Tech. Dr. Rangarajan Dr. Sakunthala Engineering College, Chennai. His research interests include antennas and electromagnetism.. He has ten years' teaching and 7 years' research experience. His ORCID is 0000-0003-2908-7069.

S. Ramesh is a Professor with 19 years' teaching experience at SRM Valliammai Engineering College in Chennai. He is a senior member of the IEEE Antennas & Propagation Society (S'10-M'17-SM'18) His research interests include antennas, propagation. His ORCID is 0000-0002-2946-5296.

Parthasarathy Ramanujam is an Assistant Professor at the National Institute of Technology, Tiruchirappalli. His research interests include microwave components and circuits His ORCID is 0000-0003-3179-0036.

E. Manikandan is a Senior Assistant Professor at the Centre for Innovation and Product Development and School of Electronics Engineering at Vellore Institute of Technology, Chennai. His research interests include antennas, micromachining and sensors. His ORCID is 0000-0002-0381-6406.